Structure
Article

The Structure of *Lethocerus* Troponin C: Insights into the Mechanism of Stretch Activation in Muscles

Gianfelice De Nicola,[1] Christoph Burkart,[2,5] Feng Qiu,[3,6] Bogos Agianian,[3,7] Siegfried Labeit,[4] Stephen Martin,[1] Belinda Bullard,[2,3] and Annalisa Pastore[1,*]
[1] Molecular Structure Division, National Institute for Medical Research, The Ridgeway, Mill Hill, London NW7 1AA, United Kingdom
[2] Department of Biology, University of York, York YO10 5DD, United Kingdom
[3] European Molecular Biology Laboratory, Meyerhofstrasse 1, D-69117 Heidelberg, Germany
[4] Institut für Anästhesiologie und Operative Intensivmedizin, Universitätsklinikum Mannheim, D-68167 Mannheim, Germany
[5] Present address: The Scripps Research Institute, 10550 Torrey Pines Road, La Jolla, CA 92037, USA.
[6] Present address: Center for Advanced Biotechnology and Medicine, UMDNJ-Robert Wood Medical School, 679 Hoes Lane, Piscataway, NJ 08854, USA.
[7] Present address: Department of Molecular Biology and Genetics, Democritus University of Thrace, Dimitras 19, 68100 Alexandroupolis, Greece.
*Correspondence: apastor@nimr.mrc.ac.uk
DOI 10.1016/j.str.2007.05.007

SUMMARY

To gain a molecular description of how muscles can be activated by mechanical stretch, we have solved the structure of the calcium-loaded F1 isoform of troponin C (TnC) from *Lethocerus* and characterized its interactions with troponin I (TnI). We show that the presence of only one calcium cation in the fourth EF hand motif is sufficient to induce an open conformation in the C-terminal lobe of F1 TnC, in contrast with what is observed in vertebrate muscle. This lobe interacts in a calcium-independent way both with the N terminus of TnI and, with lower affinity, with a region of TnI equivalent to the switch and inhibitory peptides of vertebrate muscles. Using both synthetic peptides and recombinant proteins, we show that the N lobe of F1 TnC is not engaged in interactions with TnI, excluding a regulatory role of this domain. These findings provide insights into mechanically stimulated muscle contraction.

INTRODUCTION

Muscle contraction is regulated by the periodic fluctuation of calcium concentration, which activates contraction and triggers an increase in force. Ca^{2+}-promoted regulation is almost exclusively achieved by subtle differences in the sequence of a single molecule, troponin C (TnC). This protein is part of the troponin (Tn) complex, together with TnT, which anchors the complex to the thin filament through interactions with tropomyosin, and TnI, which is responsible for inhibiting the myosin ATPase cycle (Greaser and Gergely, 1971; Gordon et al., 2000). According to the steric blocking model, Ca^{2+} binding to TnC results in movement of tropomyosin from a blocking position on actin to one in which myosin binding sites are exposed (Vibert et al., 1997; Gordon et al., 2000; Mak and Smillie, 1981; Potter et al., 1995). TnC contains four EF hand motifs assembled in pairs to form two globular domains, the so-called N and C lobes (Kretsinger, 1976). Although evolved as Ca^{2+}-binding motifs, the number of active EF hands in TnC and their positions in the protein are different in different species or isoforms. In most species, the C lobe, which contains up to two high-affinity Ca^{2+} binding sites, is permanently occupied by either Mg^{2+} or Ca^{2+} and is responsible for anchoring TnC to the rest of the troponin complex (for a review, see Gagné et al., 1998). In vertebrate TnC, the N lobe is able to bind either one or two Ca^{2+} ions, depending on whether it is in cardiac or skeletal muscle, respectively. In skeletal muscle TnC, Ca^{2+} binding induces a conformational transition in the N lobe from a closed structure, in which the four helices are almost parallel to each other, to an open state, which causes exposure of the hydrophobic patch and allows binding of the domain to the "switch peptide" of TnI (residues 115–131) (Mercier et al., 2003). In cardiac muscle, in which the N lobe of TnC has only one Ca^{2+}-binding site, Ca^{2+} is unable to induce the conformational transition. Opening of the domain occurs, but only upon complex formation (Li et al., 1999, 2000).

This mechanism is further complicated in insect muscle. One of the most striking features of insects is the ability of some species to contract the flight muscles at very high frequencies. To adapt to this requirement, indirect flight muscles (IFMs) have evolved two distinct forms of activation which are finely tuned to the type of movement required (Agianian et al., 2004; Linari et al., 2004): a stretch-activated mechanism (asynchronous contraction) is used for flying, whereas Ca^{2+} regulation is important during the "warm-up" contractions which precede flight in large insects (synchronous contraction).

In asynchronous muscles, there is no direct correspondence between nerve impulses and contractions. The muscles are stimulated by periodic mechanical stretches at a constant low concentration of Ca^{2+}, which is

maintained in the muscle by intermittent nerve stimulation. Alternate stretch activation of opposing sets of IFMs produces oscillations in the thorax, which moves the wings (Pringle, 1949). This type of activation enables the wings to beat at frequencies that are higher than can be achieved by stimulating individual contractions in the muscles with Ca^{2+} pulses produced by nerve stimulation. IFMs can also be stimulated to contract synchronously with nerve impulses; this produces a tetanus at higher frequencies but is not used during flight.

In asynchronous flight muscles, there are two isoforms of TnC, F1 and F2 (Qiu et al., 2003). F1 TnC is responsible for activating the muscle following a stretch, whereas F2 produces a sustained contraction, the size of which depends on the concentration of Ca^{2+} in the fiber. F1 TnC has an N lobe that is completely insensitive to Ca^{2+}, whereas the N lobe of F2 TnC was demonstrated to contain one Ca^{2+}-binding EF hand. During flight, stretch activation and Ca^{2+} activation are finely balanced, depending on the Ca^{2+} concentration produced by the intermittent nerve impulses (Agianian et al., 2004; Linari et al., 2004; Gordon and Dickinson, 2006).

Although there is some understanding of Ca^{2+}-regulated contraction, very little is known about the structural bases of stretch activation. It is, for instance, still unclear whether the unique Ca^{2+} bound to the C lobe is sufficient to promote domain opening of this C lobe and whether the N lobe has a regulatory role. Yet, finding an answer to these questions is essential to understand not only insect flight but, more generally, the way muscle regulation has evolved in different species.

Here we have focused on the F1 TnC isoform from *Lethocerus* with the aim of providing new insights into mechanical activation of contraction. This giant water bug has often been used as a model system to study and compare the mechanisms of synchronous and asynchronous contraction because it is easy to manipulate. We have solved the structure in solution of Ca^{2+}-loaded (holo) F1 TnC using nuclear magnetic resonance (NMR) techniques. The structural determinants were compared with those of different species. We have also characterized the mode of binding of holo and apo F1 TnC to TnH (the *Lethocerus* ortholog of TnI) both by using short synthetic peptides and by reconstructing the F1 TnC/TnH complex. Our study provides, to our knowledge, the first description of the structure of the muscle component essential for stretch activation.

RESULTS

Description of the Holo F1 TnC Structure

The solution structure of holo F1 TnC was solved by standard high-resolution NMR methods (Table 1). It consists of a typical EF hand fold with two globular domains spaced by a flexible linker (Figure 1A). The two domains superpose independently with a backbone root-mean-square deviation of 0.8 Å. Each domain consists of two EF hand motifs, each of which comprises two α helices flanking the 11 residue loop which, in Ca^{2+}-active EF hands, contains the six ligands responsible for Ca^{2+} coordination. The two loops form the typical short antiparallel β sheet which keeps the two EF hands side by side. The N helix which precedes the A helix is short and is formed only in some of the members of the structure bundle.

The way the two lobes are connected has attracted much debate. In some of the known structures, the linker between the two lobes is a straight helix, which confers a dumbbell shape to the protein (Herzberg and James, 1985; Houdusse et al., 1997; Satyshur et al., 1988), whereas in others and in solution, the linker is unstructured so that the relative orientation of the two lobes is not well defined (Blumenschein et al., 2005; Dvoretsky et al., 2002; Slupsky and Sykes, 1995; Sia et al., 1997; Vinogradova et al., 2005). In the solution structure of *Lethocerus* F1 TnC, the linker is unstructured and highly flexible allowing the two lobes to tumble independently, as also shown by the relaxation data (Figure 1B).

The Apo N and Holo C Lobes of F1 TnC Are in a Closed and Open Conformation, Respectively

An important question is whether the two lobes are in a closed or open conformation and whether these states are modulated by Ca^{2+} and/or by binding to TnI/TnH. Comparison between the interhelical angles of each of the two lobes in the holo F1 structure shows that the overall arrangement of the four helices in the N lobe is in a closed conformation, whereas the C lobe is in an open state. Although finding a closed conformation of the N lobe is not entirely surprising as this conformation is usually observed in apo EF hands (Yap et al., 1999), the C lobe shows a novel feature: a single Ca^{2+} ion is enough to induce opening of the domain.

Interestingly, submission of the N lobe of F1 TnC to the SSM server (http://www.ebi.ac.uk/msd-srv/ssm/) against the Protein Data Bank (PDB) database picks up with the highest score the structure of the apo N lobe of skeletal TnC, which is in the closed conformation (PDB code: 1skt; Tsuda et al., 1999) (Figure 2A). The C lobe shares the highest similarity with the holo C lobe of human cardiac TnC in complex with the inhibitory region of TnI (PDB code: 1ozs; Lindhout and Sykes, 2003). This strongly indicates that in its Ca^{2+}-bound state the C lobe of F1 TnC is already arranged to interact with TnH.

Does the C Lobe of F1 TnC Undergo a Conformational Transition upon Ca^{2+} Binding?

To test the possibility that the C lobe could already be in an open conformation when in the Ca^{2+}-free state, we compared two $\{^{1}H,^{15}N\}$-HSQC spectra recorded in the presence and absence of Ca^{2+}. The stoichiometry previously estimated by atomic absorption (Qiu et al., 2003) and mass spectrometry (Agianian et al., 2004) and the identity of the Ca^{2+} binding site on F1 TnC are fully in agreement with the NMR spectrum (Figure 2B): the ^{15}N chemical shift of the amido nitrogen of the residue in position 8 of a canonical EF hand loop is highly diagnostic of the presence of Ca^{2+} binding, thus providing direct identification of the

Table 1. Structural Statistics of *Lethocerus* F1 TnC

Final NMR Restraints	
Total distance restraints	3840
Unambiguous/ambiguous	3401/439
Intraresidue	1578
Sequential	840
Medium (residue i to i + j, j = 2 − 4)	573
Long-range (residue i to i + j, j > 4)	849
Deviation from Idealized Geometry	
Bond lengths (Å)	0.003 ± 0.000
Bond angles (°)	0.396 ± 0.023
Improper dihedrals (°)	0.296 ± 0.023
Restraint violations	
Distance restraint violation > 0.5 Å	0
Dihedral restraint violation > 5°	0
Coordinate Precision (Å) with Respect to the Mean Structure	
Backbone of N-terminal structured regions	0.35
Heavy atoms of N-terminal structured regions	0.80
Backbone of C-terminal structured regions	0.61
Heavy atoms of C-terminal structured regions	0.95
Backbone of N-terminal secondary structure element	0.26
Heavy atoms of N-terminal secondary structure element	0.79
Backbone of C-terminal secondary structure element	0.34
Heavy atoms of C-terminal secondary structure element	0.82
Quality Checks	
WHAT IF first-generation packing quality	n.d. (−1.648)[a]
WHAT IF second-generation packing quality	−1.980 (−1.058)
WHAT IF Ramachandran plot appearance	−3.096 (−2.960)
WHAT IF $\chi1$-$\chi2$ rotamer normality	−2.557 (−2.205)
WHAT IF backbone conformation	−2.324 (−1.915)
PROCHECK most favored region (%)	83.6
Quality Checks	
PROCHECK additionally allowed regions (%)	14.4
PROCHECK generously allowed regions (%)	0.7
PROCHECK disallowed regions (%)	1.2

n.d., not determined.
[a] The numbers not in parentheses were calculated for the structure bundle after water refinement, whereas the numbers in parentheses refer to the lowest energy structure.

residues involved (Biekofsky et al., 1998). Comparison of the {^{1}H,^{15}N}-HSQC spectra of the apo and holo forms of F1 TnC shows conclusively that a single Ca^{2+} ion is accommodated in site IV of the C lobe (V144, which moves from 8.35 and 120.0 ppm to 9.89 and 128.8 ppm), while the other three coordination sites are inactive even at high (millimolar) concentrations of this cation.

Besides these chemical shifts, the two spectra do not look significantly different and both are typical of folded species, suggesting that both domains are also intrinsically structured in the absence of Ca^{2+}. A similar overall chemical shift spreading could be observed in a recombinant fragment spanning only the C-terminal lobe (see the Supplemental Data available with this article online). This is at variance with what is observed for the C lobe of skeletal muscle TnC, where the spectrum of the apo form is characterized by the low dispersion of chemical shifts, which appear to be in random coil positions (Mercier et al., 2000). Local chemical shift variations suggest that the C lobe of F1 TnC undergoes some structural rearrangement upon Ca^{2+} binding, although it is difficult to assess the extent of the conformational change in the absence of the structure of the apo form.

Thermal Stability of F1 TnC

The thermal stability of the apo and holo forms of F1 TnC were tested to understand further the differences from vertebrate TnC. Thermal unfolding curves, as recorded by circular dichroism (CD), show that the apo protein undergoes a highly cooperative transition with an apparent melting point around 50°C (Supplemental Data). If, however, the curve is fit with a single-component fit model, a poor chi-square value is found (2.34), suggesting the presence of a two-step unfolding. When assuming a two-component fit, the chi-square value is 1.03. The melting temperatures for the two-component fit are 37.5°C and 62.4°C.

Holo F1 TnC undergoes instead an apparent single transition at a temperature of 56.5°C, indicating that Ca^{2+} stabilizes the C lobe and leads to an unfolding temperature comparable to that of the N lobe.

These results indicate that, although the apo C lobe is folded at room temperature, it has a significantly lower stability than the N lobe. The difference is reduced in the holo form.

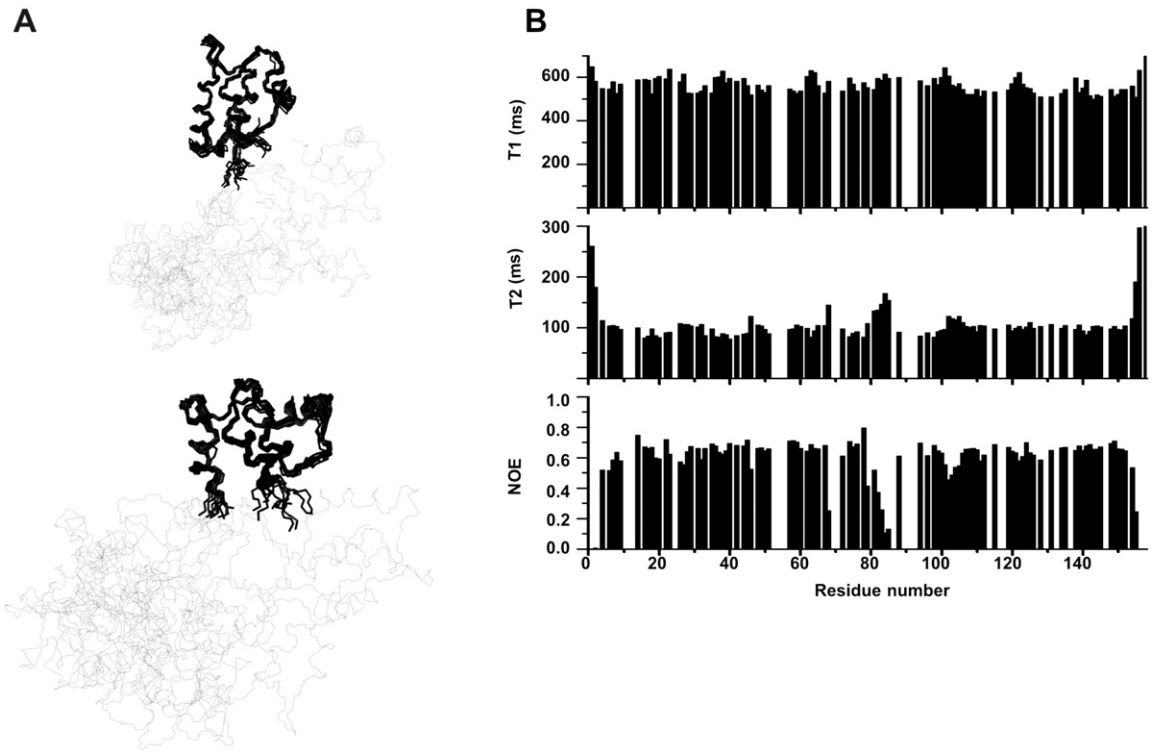

Figure 1. Solution Structure of Holo F1

(A) The three-dimensional fold of F1 represented by the NMR bundle. The 20 lowest-energy structures of F1 resulting from ARIA calculations, after energy minimization in a shell of water, are displayed.

(B) Relaxation parameters of the backbone ^{15}N nuclei plotted as a function of the residue number. The data were recorded at 25°C and 500 MHz.

The Switch Peptide of Insect TnI Is Highly Divergent from the Vertebrate Sequence

We used the structural information gained on F1 TnC to characterize the interactions of holo and apo F1 TnC with TnH. We first determined the sequence of *Lethocerus* TnH cDNA (Figure 3A). The corresponding amino acid sequence confirmed previous work: the molecule is a TnI which shares ca. 27% identity with vertebrate TnI. This sequence is followed by a C-terminal stretch that is rich in proline and alanine (Bullard et al., 1988; Peckham et al., 1992; Qiu et al., 2003). We identified regions along the sequence that could correspond to the N-terminal region and to the inhibitory and switch peptides in vertebrate TnI, and could thus be expected to interact with the C and N lobe of TnC, respectively. Whereas the N-terminal region (30–61) and the inhibitory peptide share sufficient sequence similarity with the vertebrate sequences to suggest that their role may be conserved in *Lethocerus*, the switch peptide is shorter and highly divergent. For instance, Arg115, which is a key residue in skeletal TnI salt bridged with Glu63 and Gln84, is substituted by a serine (Ser147). Likewise, there is no conservation of the residues of TnC that should contribute to the interaction (Figure 3B).

These observations suggest a highly divergent regulation of contraction in stretch-regulated insect muscles.

F1 TnC Interacts with the Two TnH Peptides with Different Affinities and in a Ca^{2+}-Independent Way

To test this hypothesis, we designed two synthetic peptides, TnH(30–61) and TnH(126–159), which should correspond, respectively, to the N terminus and to the inhibitory and switch regions of vertebrate TnI. They were used in binding studies with both the apo and holo forms of F1 TnC. The binding constants (K_ds) of the four complexes were measured both by fluorescence and by CD spectroscopy. Affinities were first determined by competition experiments in which solutions containing both melittin and each of the peptides individually were titrated with F1 TnC. The K_d values for TnH(30–61) binding to apo and holo TnC are 1.3 ± 0.3 nM and 1.5 ± 0.5 nM, respectively, thus indicating a strong and specific interaction (Figure 4C). Lower affinities (5.4 ± 1.5 μM and 8.5 ± 3.7 μM for holo and apo TnC, respectively) were observed for the complex with TnH(126–159) (Figures 4A and 4B). These data suggest Ca^{2+}-independent binding of the peptides.

Determination of the dissociation constants for Ca^{2+} binding to TnC in the absence and presence of the peptides confirmed this hypothesis (data not shown): we expected that, if the peptides bound more strongly in the presence of Ca^{2+}, the cation should have a higher affinity for the protein in the presence of the peptide. Ca^{2+} K_ds were instead largely comparable, being 0.62 ± 0.06 μM

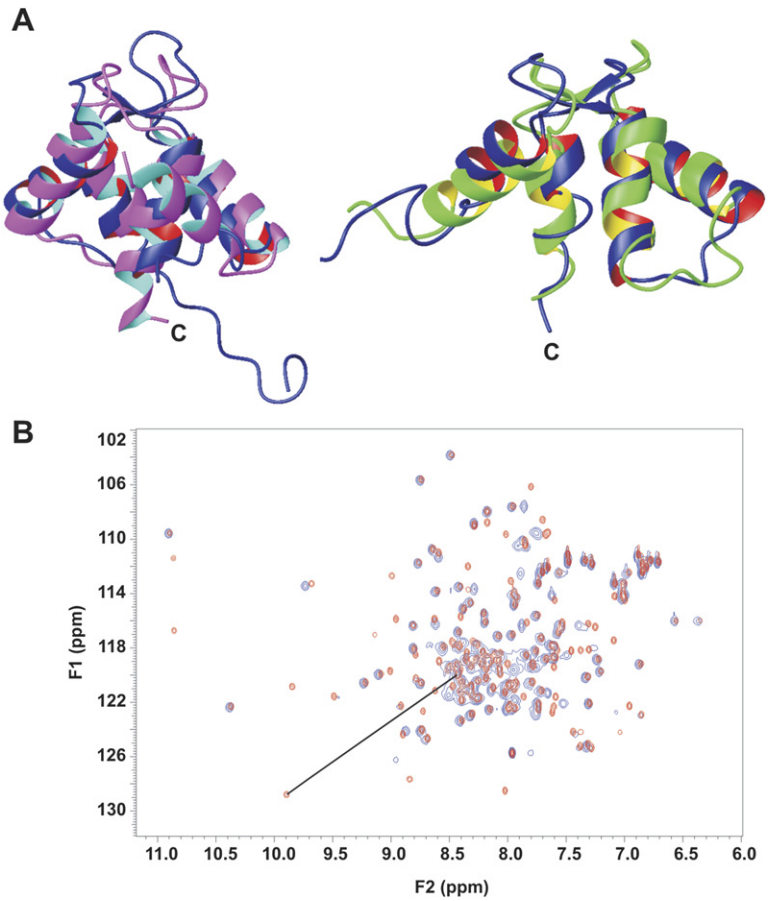

Figure 2. Conformational Status of the Two Lobes of F1 TnC

(A) Structural comparison of the two lobes of F1 TnC with the PDB picks up as the highest hits the apo N lobe of skeletal TnC, which is in closed conformation (PDB code: 1skt; Tsuda et al., 1999) and the holo C lobe of cardiac TnC in complex with the corresponding N terminus of TnI (PDB code: 1ozs; Lindhout and Sykes, 2003).

(B) Comparison of the HSQC spectra of apo (blue) and holo (red) *Lethocerus* F1 TnC. The spectra were recorded at 25°C on a 600 MHz spectrometer. The shift upon Ca^{2+} addition of the resonance of V144 is indicated.

(in the absence of the peptide), 0.66 ± 0.08 μM (in the presence of an excess of TnH[30–61]), and 0.42 ± 0.05 μM (with an excess of TnH[126–159]).

To have an independent measurement of the K_d of TnH(126–159), which has lower affinity, we studied its effects on the stability of the C lobe of apo F1 TnC to both thermal and chemical denaturation (data not shown). In thermal denaturations, the midpoint for unfolding of the C lobe of apo TnC increased from 37.5°C to 52.8°C in the presence of an excess of TnH(126–159), whereas the increase was from 56.5°C to 62.7°C for holo TnC. As higher temperatures are expected to stabilize hydrophobic interactions, the observed increases indicate that the interaction is in both cases mostly of hydrophobic nature. Analysis of the urea unfolding experiments using the linear extrapolation model gave a difference of binding free energy ΔG^0 and ***m*** values of 1.37 ± 0.12 kcal/mol and −1.13 ± 0.04 kcal/(mol.M) in the absence of TnH(126–159). In the presence of the peptide, the ΔG^0 values increased to 2.29 ± 0.04 (for 58 μM peptide) and 2.81 ± 0.05 (for 170 μM peptide). These increases in stability are consistent with dissociation constants in the range of 10–15 μM (Masino et al., 2000).

Finally, the far-UV CD spectra of the complexes of apo and holo TnC with TnH(126–159) are significantly more intense (higher α-helical content) than the sum of the appropriate component spectra (data not shown). We thus performed titrations of TnC with TnH(126–159) in which we monitored the far-UV CD signal change accompanying complex formation. Although the relatively high concentrations required for these experiments did not permit determination of precise K_d values, they clearly showed that the interaction is of similar strength in the presence and absence of Ca^{2+}.

Taken together, these results indicate that F1 TnC is able to bind both peptides in vitro but with appreciably different affinities and that the interactions are Ca^{2+} independent.

The N Lobe of F1 TnC Is Not Involved in Interactions with TnH

Direct mapping of the surface of interaction into the F1 TnC structure was obtained by NMR chemical shift perturbation following the titrations of holo and apo F1 TnC with each of the peptides (Figure 5A). For the holo and apo F1 TnC/TnH(30–61) complexes, the chemical shift variations fall into the slow exchange rate limit: both the bound and unbound species are visible with intensities that are proportional to the concentrations of the two species in solution, in agreement with a tight interaction. The pattern of chemical shift perturbation in F1 TnC/TnH(126–159) complexes is consistent instead with a fast exchange regime in the NMR timescale, in agreement with what is expected for interactions in the μM range: at each titration point, a single

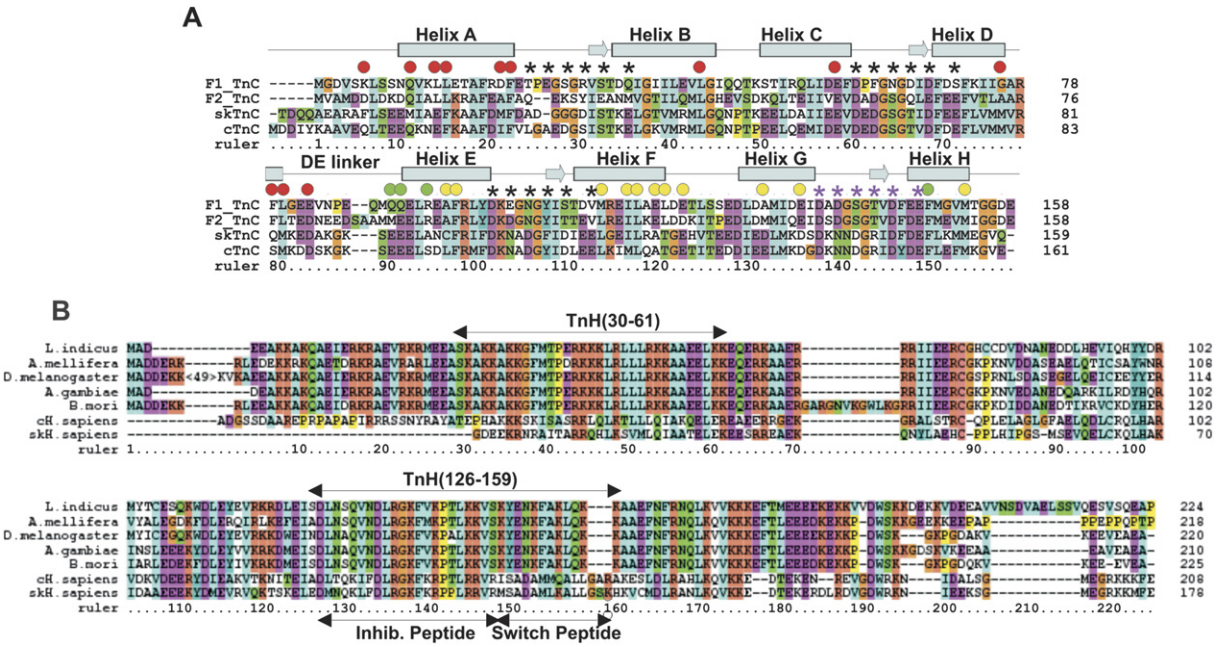

Figure 3. Alignments of the TnC and TnI Sequences of Different Muscle Isoforms and Species

(A) TnC sequence alignment in which the secondary structure elements, as observed in *Lethocerus* F1 TnC, and the position of the DE linker are indicated. Red spots indicate residues that interact with the switch peptide in skeletal Tn, green spots indicate those involved in the interaction between the DE linker and the inhibitory regions, and yellow spots indicate the residues of the C lobe involved in the interaction with the N terminus of TnI. Asterisks indicate the positions that take part in Ca^{2+} binding in canonical EF hands (Kretsinger, 1976). Only the last EF hand (indicated with magenta asterisks) is active in F1 TnC.

(B) Insect TnI sequences are compared with those from vertebrates. The positions of the peptides used in this study are indicated. The region corresponding to the switch peptide is highly divergent in insects compared to vertebrates. The *Lethocerus* TnH sequence is truncated at the end of the region homologous to vertebrate TnI; the full-length sequence is 484 residues. The GenBank/EMBL accession number of *Lethocerus* TnH is AJ621044.

crosspeak is observed at a chemical shift that is the weighted average of the bound and unbound species.

In all experiments, the residues perturbed are practically the same and all belong to the C lobe of F1 TnC (see Supplemental Data). No detectable effects are observed on the resonances of the N lobe. These results, together with the appreciable difference between the K_d values of the two peptides with holo F1 TnC, strongly suggest that

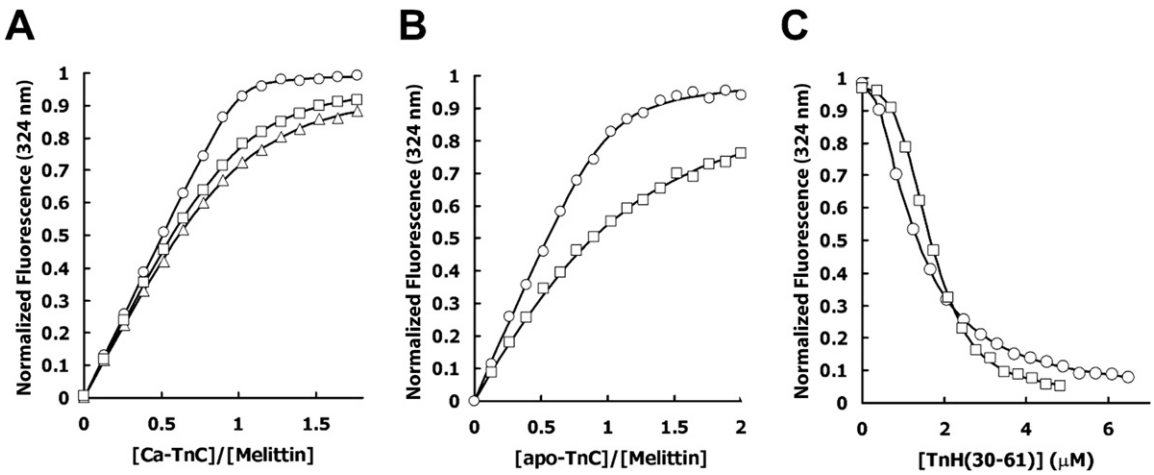

Figure 4. Probing the Interactions of Synthetic Peptides Spanning the TnI Sequence

(A) Titration of melittin (0.65 μM) with holo F1 TnC in the absence (circles) and presence of 37.5 (squares) or 75 μM (triangles) TnH(126–159).

(B) Titration of melittin (0.65 μM) with apo F1 TnC in the absence (circles) and presence (squares) of 75 μM TnH(126–159).

(C) Titration of 1.6 μM melittin plus 1.9 μM holo F1 TnC (circles) or 2.4 μM apo TnC (squares) with TnH(30–61).

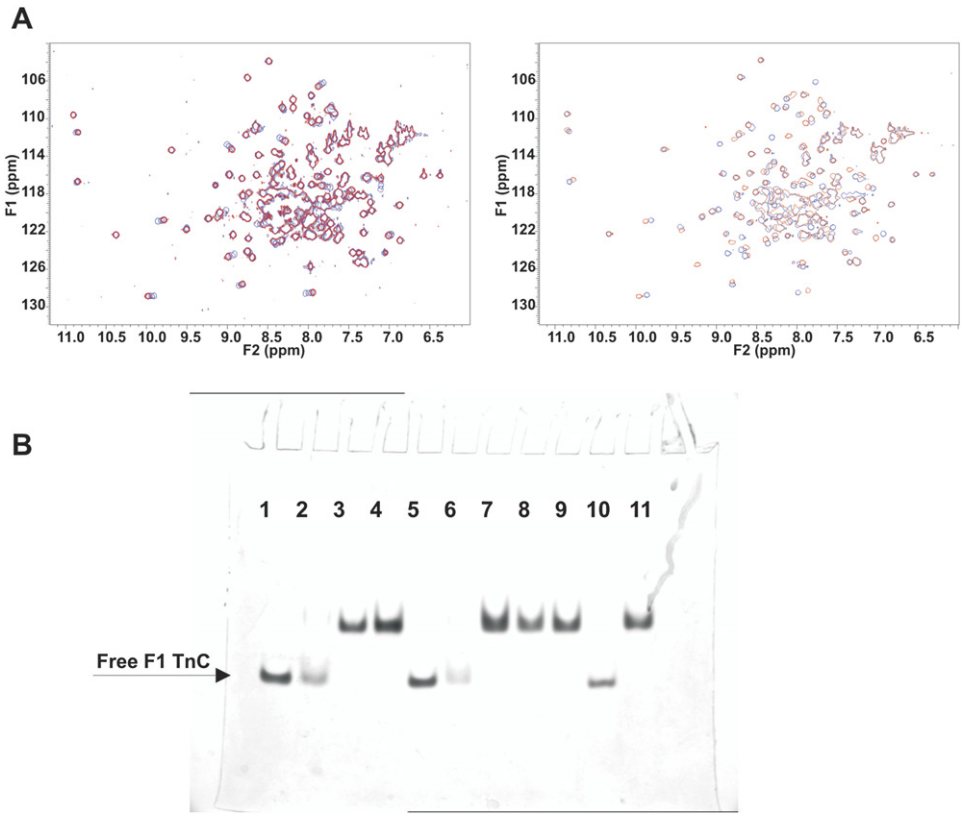

Figure 5. Testing the Interactions of TnH with F1 TnC

(A) Superposition of the HSQC spectra in the absence (blue) and presence of a molar excess (~1:3) of peptides (red). The spectra correspond to the interaction of TnH(30–61) (right panel) and TnH(126–159) (left panel). The spectra were recorded at 25°C and 600 MHz.

(B) Native gel to test the interactions of F1 TnC with the two TnH peptides. The two peptides were incubated individually or together with 22 μM F1 TnC. The lanes correspond as follows: lanes 1, 5, and 10 are controls in which the isolated F1 TnC was used; lane 2: addition of 22 μM TnH(126–159); lane 3: addition of 22 μM TnH(30–61); lanes 4 and 8: addition of an equimolar mixture of the two peptides; lane 6: addition of 66 μM TnH(126–159); lane 7: addition of 66 μM TnH(30–61). In lane 9, 22 μM TnH(30–61) and 111 μM TnH(126–159) were added. Lane 11 is the same as lane 9 but without bromophenol blue.

they compete for the C lobe of F1 TnC but neither of them has sufficient affinity for interacting with the N lobe even at high concentration.

To support this hypothesis further, we ran a native gel using F1 TnC and each of the two peptides individually or a mixture of the two (using a 1:3 molar TnH[30–61]:TnH[126–159] ratio). We observed complex formation by band shift with TnH(30–60) (Figure 5B). The complex with TnH(126–159) is probably too labile and produced a smear on the gel. As a result, the band disappeared. The complex formed in the presence of both peptides runs at the same molecular weight as the one with isolated TnH(30–61), suggesting that TnH(126–159) has no significant affinity for isolated F1 TnC when the C lobe of the protein is blocked with TnH(30–61).

Modeling a TnC/TnH(30–61) Complex

To obtain a visual impression of the TnC/TnH(30–61) complex, we built a model by homology. We first superposed the structures of the four TnC/TnI complexes currently available on the C lobe of F1 TnC. In addition to the Ca^{2+}-loaded Tn complexes from cardiac and skeletal muscles (Takeda et al., 2003; Vinogradova et al., 2005), we compared the structure of skeletal TnC in complex with fragment 1–47 of TnI (Vassylyev et al., 1998) and the skeletal TnC apo form (Vinogradova et al., 2005). The comparison shows that, despite clear differences in the arrangement of the N lobe of TnC and of the interacting region of TnI, the mode of recognition of the C lobe involves the same groove between helices E and H and the FG loop and leads to the same local relative orientation of TnI and the C lobe of TnC (Figure 6A). This suggests that, independently of the specific sequences involved, the mode of interaction is highly conserved.

When the model was built, using the coordinates of the cardiac complex as a template (Takeda et al., 2003), we compared the network of interactions formed with those in known complexes to identify key positions and evaluate their conservation (Figure 6B). In cardiac TnI, there are five hydrophobic residues (L53, L54, I56, A57, and L61) which pack against the hydrophobic core of TnC and seem to lead the interaction. Additionally, three positively charged

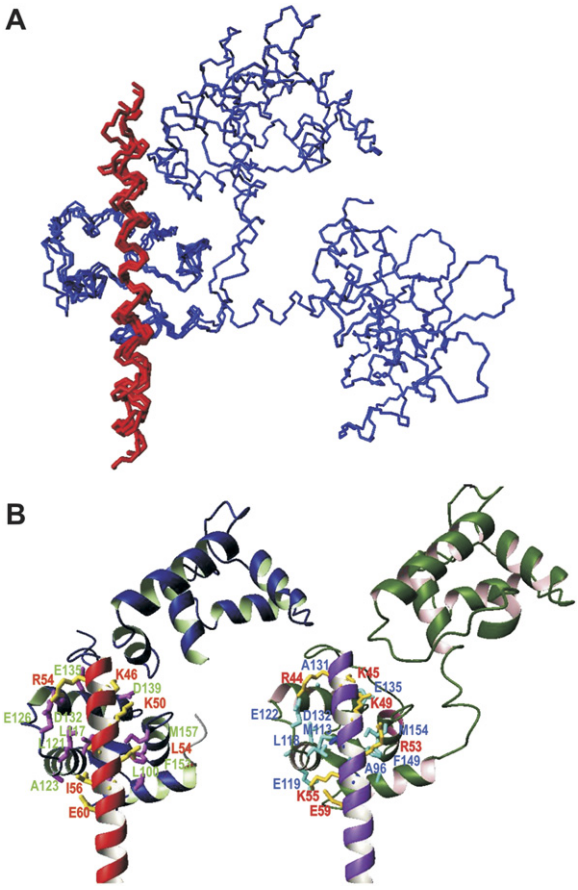

Figure 6. Modeling of the Complex

(A) Structural superposition of the four available structures of TnC complexes (PDB codes: 1a2x, 1j1d, 1ytz, and 1yv0) with the N terminus of TnI. The structures were superposed on the C lobe of TnC. The comparison shows that, despite the differences in the relative orientation of the N lobe, TnI interacts in the same groove and adopts the same relative orientation to the C lobe.

(B) Comparison of the network of interactions formed between the C lobe of TnC and TnI in the cardiac complex (Takeda et al., 2003) (left panel) and in a homology model built (right panel) using the cardiac structure (PDB code: 1j1d) as a template. The side chains of the key residues involved are displayed explicitly and labeled in red and green according to whether they correspond to TnI and TnC, respectively, for the cardiac structure. Similarly, they are colored in red and blue according to whether they correspond to *Lethocerus* TnH and TnC, respectively.

residues of TnI (R45, K46, and K50) and E60 form salt bridges with residues of opposite charge in TnC. A similar network of interactions is observed in the skeletal muscle complex (Vinogradova et al., 2005). These contacts are all semiconserved in *Lethocerus* and lead to a similar network of interactions.

Searching for Interactions between the N Lobe of TnC and TnH

Given the relatively low sequence similarity of the *Lethocerus* and vertebrate Tn sequences, it is in principle possible that other regions of TnH outside those tested could establish interactions with the N lobe of TnC. To clarify this point, two longer constructs of TnH spanning residues 1–224 and 1–340 (TnH[1–224] and TnH[1–340]) were produced as recombinant proteins. These constructs include both peptides previously tested and exclude only the low-complexity C-terminal tail of full-length *Lethocerus* TnH. Because of its highly repetitive character, it is unlikely that this region could contribute to specific binding with F1 TnC. The NMR spectra of the F1 TnC/TnH(1–224) and F1 TnC/TnH(1–340) complexes were recorded (Figures 7A and 7B). Apart from an appreciable line broadening due to the large molecular weight of the complexes, which tumble slowly, the spectra can be overlapped almost precisely with those of the smaller F1 TnC/TnH(30–61) complex.

This clearly indicates that the C lobe of F1 TnC retains the same features as observed with the peptides and confirms that the N lobe does not interact with TnH (up to residue 340).

Interaction between TnC and TnH Detected by Yeast Two-Hybrid Assays

The results were confirmed by an extensive two-hybrid screening study using different constructs of TnH and F1 TnC (Figure 7B). Full-length F1 TnC interacted with full-length TnH and with all TnH constructs having the N terminus intact. A construct spanning the isolated TnH N terminus interacted with F1 TnC. The sequence downstream of the TnI portion (residues 1–224) of TnH was unnecessary for interaction. An F1 TnC construct with a mutation in the Ca^{2+}-binding site IV interacted with the same TnH constructs as wild-type F1 TnC, showing that the interaction is independent of Ca^{2+} binding. A truncated F1 TnC lacking site IV did not bind to TnH, whereas F1 TnC with the N-terminal lobe removed, lacking sites I and II, bound to the same TnH constructs as intact F1 TnC. The PA-rich sequence at the end of TnH (TnH-P) does not interact with F1 TnC.

Therefore, the N terminus of TnH and the C-terminal lobe of F1 are necessary and sufficient for interaction of the two molecules.

DISCUSSION

The structure of F1 TnC provides, to our knowledge, the first description of the structure of one of the major components that is expected to determine asynchronous muscle contraction. Despite the obvious similarities with other TnC structures, the *Lethocerus* protein has specific features which may be related to its function. F1 TnC does not contain the N helix, having a shorter N terminus compared to other TnC sequences. This helix has been shown to increase Ca^{2+} affinity (Chandra et al., 1994). It is therefore unnecessary in the Ca^{2+}-insensitive N lobe of F1 TnC. We observe a closed conformation for the Ca^{2+}-insensitive N lobe, in agreement with what is observed in other TnCs in the absence of Ca^{2+} and, more generally, in apo EF hand domains (Gagné et al., 1998; Yap et al., 1999). More unusually, the presence of only one Ca^{2+} ion is

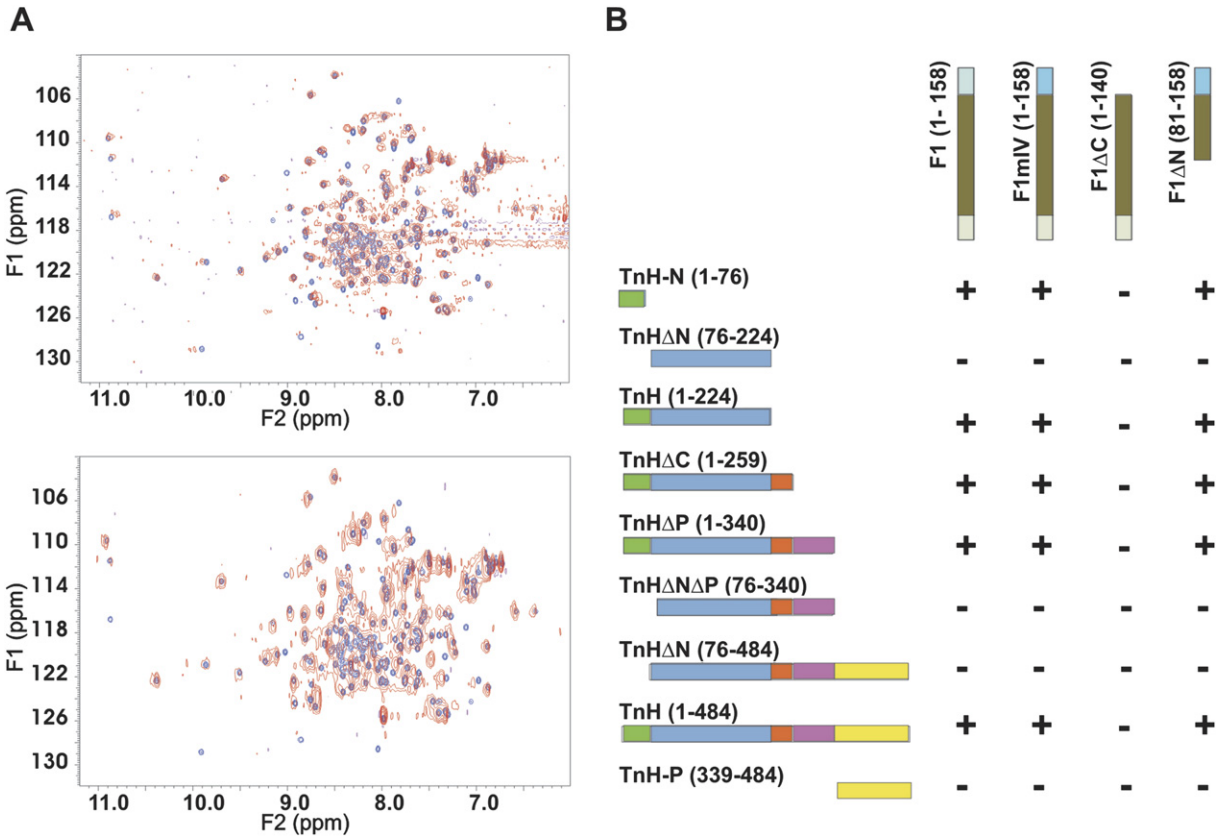

Figure 7. Searching for Regions which Could Interact with the N Lobe of F1 TnC

(A) HSQC spectra of the F1 TnC/TnH(1–224) (top) and F1 TnC/TnH(1–340) (bottom) complexes.

(B) Yeast two-hybrid assay of the interaction between F1 TnC and TnH. TnH constructs were in the bait vector and F1 TnC constructs were in the prey vector. Amino acid residue numbers of fragments are shown. F1 mIV is mutated at site IV; TnH(1–224) is the core TnI sequence with homology to vertebrate TnI. Interaction was estimated by cotransforming plasmids in yeast and observing *His3* gene activation. + indicates a strong growth of yeast, and – indicates no growth.

enough to induce an open conformation in the C lobe of F1 TnC. This is at variance with the N lobe of cardiac TnC, which also binds only one Ca^{2+} ion, but does not undergo significant structural changes upon Ca^{2+} binding (Sia et al., 1997). In cardiac muscles, Ca^{2+} binding only causes an increase in the affinity for TnI compared to the apo form, but does not induce a significant change in the structure of the unbound form. The presence of both Ca^{2+} and TnI is necessary to stabilize an open conformation, which leads to exposure of the hydrophobic pocket (Li et al., 1999). Currently, F1 TnC is the only available TnC structure in an open conformation with a single bound Ca^{2+} ion.

We also studied the dynamic behavior and stability of Ca^{2+}-loaded F1 TnC. We observed no substantial difference in protein flexibility within each of the two lobes, suggesting that they have similar dynamic properties. This is in agreement with the comparable thermal stability of the N lobe and the holo C lobe. A similar behavior and appreciably lower stability of the apo protein are also observed in skeletal TnC and in calmodulin, where the N lobe is more stable than the apo C lobe (Fredricksen and Swenson, 1996; Masino et al., 2000). The apo C lobe of F1 TnC is, however, more stable than the corresponding region in skeletal TnC, which is unfolded at room temperature (Mercier et al., 2000). As in other TnC structures, we observed high flexibility of the D/E linker. This region clearly constitutes a hinge which makes the two lobes structurally semi-independent.

Finally, we have characterized the interactions of F1 TnC with TnH using different constructs and complementary techniques. We prove conclusively that only the C lobe binds TnH in the binary complex, leaving the N lobe idle. This finding indicates that stretch activation is regulated by a mechanism that is completely different from that observed in Ca^{2+}-activated muscles, and suggests that regulation is achieved through the C lobe rather than the N lobe. A similar hypothesis was proposed for scallop troponins (Ojima et al., 2000).

The C lobe binds both the N terminus of TnH and a peptide spanning the inhibitory and switch regions. Both interactions are Ca^{2+} independent. While not expected to regulate stretch activation, the presence of an active Ca^{2+} binding loop is nevertheless essential for stretch activation

(Agianian et al., 2004). This suggests that, in muscle, a third component (likely TnT or tropomyosin) modulates the interaction of TnH with F1 TnC, increasing the difference in relative stabilities of the apo and holo complexes.

The complexes with the two peptides differ greatly in their affinities. The interaction with the TnH N terminus is in the nanomolar range, which is comparable to the value reported for the skeletal TnC/TnI complex (Tripet et al., 2003). The K_d of the TnC/TnH(126–159) complex is in the micromolar range, as in the complex of skeletal TnI(96–111) with the C lobe of TnC (Mercier et al., 2000). Could the two complexes be alternately formed during muscle contraction? A model in which two regions of TnI compete for the C lobe of TnC was already proposed for skeletal muscle (Tripet et al., 1997). This hypothesis was, however, subsequently discredited by the identification of a second site of weaker interaction on the C lobe and by structure determination of the Tn complex (Vinogradova et al., 2005). To check whether a similar situation could occur in *Lethocerus*, we repeated the experiment proposed by Tripet et al. (2003) based on a native gel. We did not observe an additional band shift in the presence of both peptides, as expected if both interactions were possible at the same time. It therefore remains possible that competition between two distinct regions of TnH, which occupy the C lobe of TnC alternately, could be the basis of stretch activation. Much more work will be needed to acquire a full description of all the components and to provide an atomic model of stretch activation.

EXPERIMENTAL PROCEDURES

Sequencing of *Lethocerus* TnH cDNA

TnH cDNA was sequenced as previously described (Qiu et al., 2003). A positive clone was obtained by screening a *Lethocerus* λgt11 expression library with monoclonal antibodies to TnH (MAC 81, 143, 144, and 195) (Bullard et al., 1988). Primers were designed from the sequence of the insert and used for rapid amplification of cDNA ends (RACE) with IFM cDNA. Primers were: 5′-GCACACGGATAAAAACACGGAGG-3′ for 5′ RACE and 5′-CCGCGGAAGGCGCAGCTCCACCGGCGG-3′ for 3′ RACE; full-length cDNA was amplified by PCR from 5′ and 3′ RACE ends, and sequenced.

Sample Preparation

Lethocerus F1 TnC cDNA in a pET-M11 vector (Stratagene) was expressed in *Escherichia coli* BL21(DE3)pJY2 cells according to Qiu et al. (2003). Samples containing H_2O:D_2O (9:1 v/v) solutions with 0.9 mM protein in 100 mM KCl (pH 6.8) and 5–10 equivalents of Ca^{2+} added as $CaCl_2$ were used for NMR measurements. The apo form was obtained by decalcifying the protein using the chelex100 resin (Sigma) and adding 5 mM EDTA to the solution.

The two *Lethocerus* TnH cDNA constructs, TnH(1–224) and TnH(1–340), were amplified by PCR using full-length TnH cDNA in a pCRII vector as a template and then cloned into a pET-M11 expression vector. Protein was expressed in *E. coli* BL21(DE3)RP cells, grown for 24–50 hr at 18°C–24°C. Protein derived from both constructs was in inclusion bodies. The insoluble pellet of lysed cells was dissolved in 8 M urea, 50 mM Na phosphate buffer (pH 8.0), 10 mM imidazole, 2 mM β-mercaptoethanol, and purified on an Ni-NTA agarose column (QIAGEN). Protein was eluted in the same buffer with 200 mM imidazole, and then dialyzed against 0.5 M NaCl, 20 mM Tris-HCl (pH 8.0), 2 mM β-mercaptoethanol and concentrated by precipitating with 60% saturated $(NH_4)_2SO_4$. Precipitated protein was taken up in 1–3 ml of 6 M urea, 20 mM Tris-HCl (pH 8), 4 mM DTT. The yields from 6 liters of cell culture were 54 mg of TnH(1–224) and 18 mg of TnH(1–340).

The peptides were purchased from Graham Bloomberg (Bristol University, UK) and from Pepceuticals Ltd. (Nottingham, UK). The peptide purity was over 90% as established by HPLC. The sequences were verified using MALDI mass spectrometry.

NMR Data Acquisition

The strategy adopted to obtain virtually full spectral assignment was previously described (De Nicola et al., 2004). All the experiments were recorded at 25°C. Distance restraints were derived from a 3D ^{15}N edited NOESY-HSQC and a ^{13}C edited NOESY-HSQC (100 ms mixing times), acquired on Varian Inova instruments operating at 600 and 800 MHz, respectively. The heteronuclear Overhauser effect (NOE) and the longitudinal (T_1) and transversal (T_2) relaxation rates were measured on a Varian Inova 500 MHz spectrometer. Standard pulse sequences were used. The relaxation rates were obtained by nonlinear least-squares fitting of the peak intensities to an exponential function.

Structure Calculations and Analysis

The NOESY crosspeaks were manually peak picked and the volumes were determined by the maximum integration method in XEASY (Bartels et al., 1995). The frequency tolerance was ±0.03 in the acquisition dimension, ±0.04 in the indirect proton dimension, and ±0.5 in the carbon dimension for the ^{13}C edited NOESY, while it was ±0.05, ±0.05, and ±0.5, respectively, for the ^{15}N edited NOESY. A list of dihedral angle restraints was obtained from Talos (Cornilescu et al., 1999).

Structure calculations were carried out with the ARIA 1.2 package (Linge et al., 2003), based on a standard simulated annealing CNS protocol (Brünger et al., 1998). A typical run consisted of nine iterations. The initial structure ensemble was generated at iteration 0 choosing an NOE violation tolerance and a partial assignment cutoff probability of 1000 Å and 1.01, respectively. No NOE distance restraints are excluded in this way and the partial NOE assignment is based on chemical shifts only. In the following eight iterations, as the structures improve, the NOE violation tolerances were progressively reduced (1000.0, 1.0, 0.5, 0.1, 1.0, 0.1, 0.1, and 0.1 Å), with the exception of iteration 5, in which the violation tolerance was increased to 1 Å to ensure that important NOEs consistent with the structure at that stage were not excluded. The partial assignment cutoff probability was reduced in parallel (0.9999, 0.999, 0.99, 0.98, 0.96, 0.93, 0.90, and 0.80) to eliminate ambiguous NOEs which do not contribute significantly. Twenty structures were calculated at each iteration. Floating assignment of prochiral groups and correction for spin diffusion were applied (Folmer et al., 1997; Linge et al., 2004). The best seven structures in terms of lowest global energy were selected at the end of each iteration and used in the following iteration for the assignment of additional NOEs. In the ninth iteration, the structures were refined by molecular dynamics simulation in water (Linge et al., 2003). The best 20 structures in energetic terms were selected as representative of the F1 TnC structure and used for statistical analysis.

The overall quality of the structure was inspected using the PROCHECK (Laskowski et al., 1996) and WHAT IF (Vriend, 1990) software packages. The coordinates were deposited in the PDB (PDB code: 2jnf).

Spectroscopic Measurements

Absorbance measurements were carried out with a Jasco V-550 UV/vis spectrophotometer. Uncorrected fluorescence emission spectra were recorded using a SPEX FluoroMax fluorimeter with excitation and emission bandwidths of 1.7 and 5 nm, respectively. Intrinsic tryptophan fluorescence could not be used, as none of the components contains a tryptophan residue. The K_d values of the different complexes were estimated using competition experiments with the 26 residue peptide melittin. This peptide, which contains a tryptophan in position 19, forms high-affinity 1:1 complexes both with apo and holo TnC, which produce a blue shift and an intensification of the tryptophan fluorescence. The affinities of melittin for holo and apo TnC

were determined to be 5.2 ± 1.2 nM and 26 ± 7 nM, respectively. The affinities for TnH(126–159) were determined by competition experiments in which solutions containing both melittin and TnH(126–159) were titrated with TnC, whereas for TnH(30–61) they were determined using displacement experiments in which the peptide was titrated into a solution containing the TnC/melittin complex (see Martin and Bayley, 2002 for details).

Far-UV CD spectra were recorded on a Jasco J-715 spectropolarimeter. Thermal denaturation was followed by monitoring the far-UV CD signal at 222 nm while changing the temperature from 2°C to 95°C at 1 degree/min. Chemical denaturation was followed by monitoring the far-UV CD signal at 222 nm. Titrations were performed by adding aliquots of protein in concentrated urea (10 M) to a solution of the protein at the same concentration in aqueous buffer. All measurements were made at 20°C (unless otherwise noted) in 25 mM Tris-HCl, 100 mM NaCl (pH 6.8) with added Ca^{2+} (250 μM) or EGTA (1 mM) where necessary.

Ca^{2+} Binding Studies

Ca^{2+} dissociation constants for F1 TnC in the presence and absence of the TnH peptides were determined from Ca^{2+} titrations of apo protein samples performed in the presence of the chromophoric Ca^{2+}-chelator 5,5′-dibromo-BAPTA. The dissociation constants were obtained from nonlinear least-squares fits directly to the experimentally observed titration curves. The equilibrium dissociation constant for the binding of Ca^{2+} to 5,5′-dibromo-BAPTA under the buffer conditions employed in this study was determined to be 1.8 ± 0.1 μM.

NMR Titrations

The concentrations of highly concentrated stock solutions of the peptides, in 100 mM KCl and 20 mM Tris-HCl, were measured in triplicated copies by amino acid analysis. The pH was adjusted to 6.8 with small additions of a 0.01 M NaOH solution. The pH was checked after the final peptide addition to make sure that it had remained constant throughout the titration. Complex formation was probed by recording ^{1}H-^{15}N HSQC spectra acquired at 600 MHz either on a Varian Inova or on an Advanced Bruker spectrometer equipped with a cryoprobe. The final F1 TnC/TnH(30–61) and TnC/TnH(126–159) molar ratios were 1:3 and 1:2.5, respectively.

To prepare the F1 TnC/TnH(1–224) and TnC/TnI(1–340) complexes, both components were dissolved in 8 M urea, mixed, and then refolded by gradually eliminating urea by dialysis. The final molar ratio F1 TnC/TnH(1–224) was approximately 1:1.5. The buffer composition was 20 mM Tris-HCl (pH 6.8) and either 200 mM or 500 mM KCl for the F1 TnC/TnH(1–224) and F1 TnC/TnH(1–340) complexes, respectively.

Molecular Modeling and Structural Analysis

The relevant sequences were aligned with ClustalX and submitted to Swiss-PdbViewer (version 3.7) (http://www.expasy.org/spdbv/). The resulting model was superposed to the templates using the SSM server (http://www.ebi.ac.uk/msd-srv/ssm/) and analyzed in detail using the graphic program Insight2 (Accelrys). The network of interactions was determined by WHAT IF (Vriend, 1990).

Yeast Two-Hybrid Studies of Protein Interactions

Lethocerus TnC and TnH cDNA constructs were amplified by PCR using full-length cDNA in pCRII or pCRT7 vectors as a template. The TnC constructs used for yeast two-hybrid assays were: F1 (residues 1–158), F1 mIV (mutated site IV), F1ΔC(1–140), and F1ΔN(81–158); these were amplified as described in Qiu et al. (2003).

The constructs of TnH were: TnH(1–484), TnH-N(1–76), TnHΔN(76–484), TnHΔN(76–224), TnHΔP(1–340), TnHΔNΔP(76–340), TnH-P(339–484), TnH(1–224), and TnHΔC(1–259). GenBank/EMBL accession numbers for full-length sequences are: AJ512939 for F1 (LiTnC4), AJ512940 for F2 (LiTnC1), and AJ621044 for TnH (TnI1).

Interactions between TnH and TnC were studied using the Matchmaker yeast two-hybrid system (Clontech). TnH constructs were cloned into the pGBKT7 bait vector that expresses proteins fused to the GAL4-DNA binding domain. F1 TnC constructs were cloned into the pGADT7 prey vector that expresses proteins fused to the GAL4-DNA activation domain. Pairs of TnH and TnC constructs were co-transformed into *Saccharomyces cerevisiae* strain AH109. Cells were grown for up to 10 days at 30°C on agar plates lacking leucine and tryptophan (SD-2). Activation of the *His3* reporter gene was determined by replating positive clones on agar lacking histidine, leucine, and tryptophan (SD-3), or histidine, leucine, adenine, and tryptophan (SD-4). Growth of yeast cells which showed interaction between bait and prey was scored on SD-3 or SD-4 plates.

Supplemental Data

Supplemental Data include four figures and can be found with this article online at http://www.structure.org/cgi/content/full/15/7/813/DC1/.

ACKNOWLEDGMENTS

The authors are grateful to Dr. Kevin Leonard for support and for making Clustal lineups, to Laura Sutherland (EMBL) for initial yeast two-hybrid assays, to Dr. David Trentham for moral support and encouragement, and to Drs. Mike Anson and Justin Molloy for helpful discussions. B.A. received a Marie Curie fellowship. B.B. acknowledges the EU 6th Framework grant Myores.

Received: March 12, 2007
Revised: May 7, 2007
Accepted: May 7, 2007
Published: July 17, 2007

REFERENCES

Agianian, B., Krzic, U., Qiu, F., Linke, W.A., Leonard, K., and Bullard, B. (2004). A troponin switch that regulates muscle contraction by stretch instead of calcium. EMBO J. *23*, 772–779.

Bartels, C., Xia, T., Billiter, N., Güntert, P., and Wüthrich, K. (1995). The program XEASY for computer-supported NMR spectral analysis of biological macromolecules. J. Biomol. NMR *6*, 1–10.

Biekofsky, R.R., Martin, S.R., Browne, J.P., Bayley, P.M., and Feeney, J. (1998). Ca^{2+} coordination to backbone carbonyl oxygen atoms in calmodulin and other EF-hand proteins: ^{15}N chemical shifts as probes for monitoring individual site Ca^{2+} coordination. Biochemistry *37*, 7617–7629.

Blumenschein, T.M.A., Stone, D.B., Fletterick, R.J., Mendelson, R.A., and Sykes, B.D. (2005). Calcium-dependent changes in the flexibility of the regulatory domain of troponin C in the troponin complex. J. Biol. Chem. *280*, 21924–21932.

Brünger, A.T., Adams, P.D., Clore, G.M., DeLano, W.L., Gros, P., Grosse-Kunstleve, R.W., Jiang, J.S., Kuszewski, J., Nilges, M., Pannu, N.S., et al. (1998). Crystallography & NMR System: a new software suite for macromolecular structure determination. Acta Crystallogr. D Biol. Crystallogr. *54*, 905–921.

Bullard, B., Leonard, K., Larkins, A., Butcher, G., Karlik, C., and Fyberg, E. (1988). Troponin of asynchronous flight muscle. J. Mol. Biol. *204*, 621–637.

Chandra, M., da Silva, E.F., Sorenson, M.M., Ferro, J.A., Pearlstone, J.R., Nash, B.E., Borgford, T., Kay, C.M., and Smillie, L.B. (1994). The effects of N helix deletion and mutant F29W on the Ca^{2+} binding and functional properties of chicken skeletal muscle troponin. J. Biol. Chem. *269*, 14988–14994.

Cornilescu, G., Delaglio, F., and Bax, A. (1999). Protein backbone angle restraints from searching a database for chemical shift and sequence homology. J. Biomol. NMR *13*, 289–302.

De Nicola, G., Biekofsky, R., Kelly, G., Agianian, B., Qiu, F., Bullard, B., and Pastore, A. (2004). Assignment of the ^{1}H, ^{13}C, and ^{15}N resonances

of holo isoform 4 of *Lethocerus indicus* troponin C. J. Biomol. NMR *29*, 461–462.

Dvoretsky, A., Abusamhadneh, E.M., Howarth, J.W., and Rosevear, P.R. (2002). Solution structure of calcium-saturated cardiac troponin C bound to cardiac troponin I. J. Biol. Chem. *277*, 38565–38570.

Folmer, R.H., Hilbers, C.W., Konings, R.N., and Nilges, M. (1997). Floating stereospecific assignment revisited: application to an 18 kDa protein and comparison with J-coupling data. J. Biomol. NMR *9*, 245–258.

Fredricksen, R.S., and Swenson, C.A. (1996). Relationship between stability and function for isolated domains of troponin C. Biochemistry *35*, 14012–14026.

Gagné, S.M., Li, M.X., McKay, R.T., and Sykes, B.D. (1998). The NMR angle on troponin C. Biochem. Cell Biol. *76*, 302–312.

Gordon, S., and Dickinson, M.H. (2006). Role of calcium in the regulation of mechanical power in insect flight. Proc. Natl. Acad. Sci. USA *103*, 4311–4315.

Gordon, A.M., Hornsher, E., and Regnier, M. (2000). Regulation of contraction in striated muscle. Physiol. Rev. *80*, 853–924.

Greaser, M.L., and Gergely, J. (1971). Reconstitution of troponin activity from three protein components. J. Biol. Chem. *246*, 4226–4233.

Herzberg, O., and James, M.N. (1985). Structure of the calcium regulatory muscle protein troponin-C at 28 Å resolution. Nature *313*, 653–659.

Houdusse, A., Love, M.L., Dominguez, R., Grabarek, Z., and Cohen, C. (1997). Structures of four Ca^{2+}-bound troponin C at 2.0 Å resolution: further insights into the Ca^{2+}-switch in the calmodulin superfamily. Structure *5*, 1695–1711.

Kretsinger, R.H. (1976). Calcium-binding proteins. Annu. Rev. Biochem. *45*, 239–266.

Laskowski, R.A., Rullman, J.A., MacArthur, M.W., Kaptein, R., and Thornton, J.M. (1996). AQUA and PROCHECK-NMR: programs for checking the quality of protein structures solved by NMR. J. Biomol. NMR *8*, 477–486.

Li, M.X., Spyracopoulos, L., and Sykes, B.D. (1999). Binding of cardiac troponin-I147–163 induces a structural opening in human cardiac troponin-C. Biochemistry *38*, 8289–8298.

Li, Y., Love, M.L., Putkey, J.A., and Cohen, C. (2000). Bepridil opens the regulatory N-terminal lobe of cardiac troponin C. Proc. Natl. Acad. Sci. USA *97*, 5140–5145.

Linari, M., Reedy, M.K., Reedy, M.C., Lombardi, V., and Piazzesi, G. (2004). Ca-activation and stretch-activation in insect flight muscle. Biophys. J. *87*, 1101–1111.

Lindhout, D.A., and Sykes, B.D. (2003). Structure and dynamics of the C-domain of human cardiac troponin C in complex with the inhibitory region of human cardiac troponin I. J. Biol. Chem. *278*, 27024–27034.

Linge, J.P., Habeck, M., Rieping, W., and Nilges, M. (2003). ARIA: automated NOE assignment and NMR structure calculation. Bioinformatics *19*, 315–316.

Linge, J.P., Habeck, M., Rieping, W., and Nilges, M. (2004). Correction of spin diffusion during iterative automated NOE assignment. J. Magn. Reson. *167*, 334–342.

Mak, A.S., and Smillie, L.B. (1981). Structural interpretation of the two-site binding of troponin on the muscle thin filament. J. Mol. Biol. *149*, 541–550.

Martin, S.R., and Bayley, P.M. (2002). Regulatory implications of a novel mode of interaction of calmodulin with a double IQ motif target sequence from murine dilute myosin V. Protein Sci. *11*, 2909–2923.

Masino, L., Martin, S.R., and Bayley, P.M. (2000). Ligand binding and thermodynamic stability of a multidomain protein, calmodulin. Protein Sci. *9*, 1519–1529.

Mercier, P., Li, M.K., and Sykes, B.D. (2000). Role of the structural domain of troponin C in muscle regulation: NMR studies of Ca^{2+} binding and subsequent interactions with regions 1–40 and 96–115 of troponin I. Biochemistry *39*, 2902–2911.

Mercier, P., Ferguson, R.E., Irving, M., Corrie, J.E., Trentham, D.R., and Sykes, B.D. (2003). NMR structure of a bifunctional rhodamine labeled N-domain of troponin C complexed with the regulatory "switch" peptide from troponin I: implications for in situ fluorescence studies in muscle fibers. Biochemistry *42*, 4333–4348.

Ojima, T., Koizumi, N., Ueyama, K., Inoue, A., and Nishita, K. (2000). Functional role of Ca(2+)-binding site IV of scallop troponin C. J. Biochem. (Tokyo) *128*, 803–809.

Peckham, M., Cripps, R., White, D., and Bullard, B. (1992). Mechanics and protein content of insect flight muscle. J. Exp. Biol. *168*, 57–76.

Potter, J.D., Sheng, Z., Pan, B.S., and Zhao, J. (1995). A direct regulatory role for troponin T and a dual role for troponin C in the Ca^{2+} regulation of muscle contraction. J. Biol. Chem. *270*, 2557–2562.

Pringle, J.M.S. (1949). The excitation and contraction of the flight muscle of insects. J. Physiol. *108*, 226–232.

Qiu, F., Lakey, A., Agianian, B., Hutchings, A., Butcher, G.W., Labeit, S., Leonard, K., and Bullard, B. (2003). Troponin C in different insect muscle types: identification of two isoforms in *Lethocerus*, *Drosophila* and *Anopheles* that are specific to asynchronous flight muscle in the adult insect. Biochem. J. *371*, 811–821.

Satyshur, K.A., Rao, S.T., Pyzalska, D., Drendel, W., Greaser, M., and Sundaralingam, M. (1988). Refined structure of chicken skeletal muscle troponin C in the two-calcium state at 2-Å resolution. J. Biol. Chem. *263*, 1628–1647.

Sia, S.K., Li, M.X., Spyracopoulos, L., Gagné, S.M., Liu, W., Putkey, J.A., and Sykes, B.D. (1997). Structure of cardiac muscle troponin C unexpectedly reveals a closed regulatory domain. J. Biol. Chem. *272*, 18216–18221.

Slupsky, C.M., and Sykes, B.D. (1995). NMR solution structure of calcium saturated skeletal muscle troponin C. Biochemistry *34*, 15953–15964.

Takeda, S., Yamashita, A., Maeda, K., and Maeda, Y. (2003). Structure of the core domain of human cardiac troponin in the Ca^{2+}-saturated form. Nature *424*, 35–41.

Tripet, B., van Eyk, J.E., and Hodges, R.S. (1997). Mapping of a second actin-tropomyosin and a second troponin C binding site within the C terminus of troponin I, and their importance in the Ca^{2+}-dependent regulation of muscle contraction. J. Mol. Biol. *271*, 728–750.

Tripet, B., de Crescenzo, G., Grothe, S., O'Connor-McCourt, M., and Hodges, R.S. (2003). Kinetic analysis of the interactions between troponin C (TnC) and troponin I (TnI) binding peptides: evidence for separate binding sites for the 'structural' N-terminus and the 'regulatory' C-terminus of TnI on TnC. J. Mol. Recognit. *16*, 37–53.

Tsuda, S., Miura, A., Gagné, S.M., Spyracopoulos, L., and Sykes, B.D. (1999). Low-temperature-induced structural changes in the apo regulatory domain of skeletal muscle troponin C. Biochemistry *38*, 5693–5700.

Vassylyev, D.G., Takeda, S., Wakatsuki, S., Maeda, K., and Maeda, Y. (1998). Crystal structure of troponin C in complex with troponin I fragment at 2.3-Å resolution. Proc. Natl. Acad. Sci. USA *95*, 4847–4852.

Vibert, P., Craig, R., and Lehman, W. (1997). Steric-model for activation of muscle thin filaments. J. Mol. Biol. *266*, 8–14.

Vinogradova, M.V., Stone, D.B., Malanina, G.G., Kartzaferi, C., Cooke, R., Mendelson, R.A., and Fletterick, R.J. (2005). Ca^{2+}-regulated structural changes in troponin. Proc. Natl. Acad. Sci. USA *102*, 5038–5043.

Vriend, G. (1990). WHAT IF: a molecular modelling and drug design program. J. Mol. Graph. *8*, 52–56.

Yap, K.L., Ames, J.B., Swindells, M.B., and Ikura, M. (1999). Diversity of conformational states and changes within the EF hand protein superfamily. Proteins *37*, 499–507.

Accession Numbers

The coordinates of the structure of *Lethocerus* troponin C have been deposited in the Protein Data Bank under PDB code 2jnf.

